

## Article

# Degradation of Safranin O in Water by UV/TiO<sub>2</sub>/IO<sub>4</sub><sup>−</sup> Process: Effect of Operating Conditions and Mineralization

Meriem Bendjama <sup>1</sup>, Oualid Hamdaoui <sup>2,\*</sup> , Hamza Ferkous <sup>1</sup> and Abdulaziz Alghyamah <sup>2</sup>

<sup>1</sup> Laboratory of Environmental Engineering, Process Engineering Department, Faculty of Technology, Badji Mokhtar—Annaba University, P.O. Box 12, Annaba 23000, Algeria

<sup>2</sup> Chemical Engineering Department, College of Engineering, King Saud University, P.O. Box 800, Riyadh 11421, Saudi Arabia

\* Correspondence: ohamdaoui@ksu.edu.sa or ohamdaoui@yahoo.fr

**Abstract:** Hybrid advanced oxidation processes employed to degrade recalcitrant organic pollutants in water have been widely examined in recent years. In the present work, the potential of TiO<sub>2</sub>-mediated photocatalysis in the presence of the periodate anion (IO<sub>4</sub><sup>−</sup>) toward Safranin O (SO) removal from aqueous solutions was investigated. The findings revealed a high efficiency of the UV/TiO<sub>2</sub>/IO<sub>4</sub><sup>−</sup> system due to the production of more reactive radicals (•OH, IO<sub>3</sub>• and IO<sub>4</sub>•) and non-radical species (O<sub>3</sub>, IO<sub>3</sub><sup>−</sup> and IO<sub>4</sub><sup>−</sup>). Additionally, the presence of IO<sub>4</sub><sup>−</sup> as an effective electron acceptor avoids electron-hole recombination, which induces more oxidative reactions at the hole level, increasing the degradation rate of SO. Kinetically, the involvement of IO<sub>4</sub><sup>−</sup> anions in the UV/TiO<sub>2</sub> system enhanced substantially the initial rate of degradation; from 0.295 to 12.07 mg L<sup>−1</sup> min<sup>−1</sup>. The performance of both systems, i.e., UV/TiO<sub>2</sub> and UV/TiO<sub>2</sub>/IO<sub>4</sub><sup>−</sup>, was examined under different conditions such as initial dye concentration, photocatalyst loading, periodate dosage, initial solution pH, temperature and dissolved gases. The SO degradation was found to be maximized at low concentration of pollutant at the optimum loading of catalyst (0.4 g L<sup>−1</sup>). The continuous increasing in periodate concentration over the range of 0.01–3 mM improved the system reactivity with no overdose effect. Both systems seemed to be insensitive to minor variations in temperature in the range of 15–45 °C, and showed a strong dependence on initial solution pH where the degradation rates increased proportionally with pH values up to pH 10 and decreased afterwards. A slight negative effect on the photocatalytic removal yield was noted under either aeration, nitrogen or argon atmospheres in the presence of periodate (UV/TiO<sub>2</sub>/IO<sub>4</sub><sup>−</sup>), with minor enhancement under aeration for the classical system (UV/TiO<sub>2</sub>). The mineralization of the organic substrate was also monitored. The depletion of organic matter with time was measured using total organic carbon (TOC) analysis. Despite the rapid decolorization of the dye solution in the UV/TiO<sub>2</sub>/IO<sub>4</sub><sup>−</sup> system, a TOC removal efficiency of ~62% was obtained with both systems after 180 min of treatment.

**Keywords:** degradation; safranin O; UV/TiO<sub>2</sub> process; UV/TiO<sub>2</sub>/IO<sub>4</sub><sup>−</sup> process; parametric study; mineralization



**Citation:** Bendjama, M.; Hamdaoui, O.; Ferkous, H.; Alghyamah, A. Degradation of Safranin O in Water by UV/TiO<sub>2</sub>/IO<sub>4</sub><sup>−</sup> Process: Effect of Operating Conditions and Mineralization. *Catalysts* **2022**, *12*, 1460. <https://doi.org/10.3390/catal12111460>

Academic Editor: Enshirah Da'na

Received: 14 October 2022

Accepted: 15 November 2022

Published: 18 November 2022

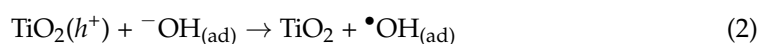
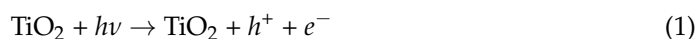
**Publisher's Note:** MDPI stays neutral with regard to jurisdictional claims in published maps and institutional affiliations.

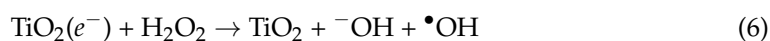
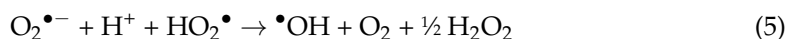


**Copyright:** © 2022 by the authors. Licensee MDPI, Basel, Switzerland. This article is an open access article distributed under the terms and conditions of the Creative Commons Attribution (CC BY) license (<https://creativecommons.org/licenses/by/4.0/>).

## 1. Introduction

Heterogeneous photocatalysis in the presence of semiconductors has been shown to be a powerful, friendly and low-cost technology for water purification [1–3]. The main step in the degradation of contaminants by photoactivated TiO<sub>2</sub> is the generation of a e<sup>−</sup>/h<sup>+</sup> pair leading to the production of powerful free radicals (Equations (1)–(6)).





Every year, textile, tanning and printing activities consume many tons of dyes and pigments to stain various products. As a result of process inefficiency, about 200,000 tons of these substances have been rejected into the environment without further treatment [4]. Synthetic dyes cause harmful effects on the environment owing to their high solubility in water, less biodegradability, their toxicity and carcinogenicity. Safranin O (SO) dye (C.I. Basic red 2) is a phenazine dye of the quinone-imine class and considered as a recalcitrant pollutant. It is commonly used in textiles, food, histology, cytology, for the biological laboratory purposes and in visible light photopolymerization [5,6]. Many processes have been applied to treat SO-containing water such as heterogeneous photocatalysis, photolysis and adsorption [5,7–12]. The photocatalytic treatment over different catalysts has presented high efficiency in SO removal. Hayat et al. [8] investigated the photodegradation of SO in an aqueous suspension of nanocrystalline  $\text{WO}_3$  locally synthesized under UV laser irradiation. They reported that the degradation over synthesized  $\text{WO}_3$  via sol–gel and precipitation techniques was faster, with an initial rate of 0.1385 and 0.2595  $\text{min}^{-1}$ , respectively, versus 0.006  $\text{min}^{-1}$  employing commercial  $\text{TiO}_2$  Degussa P25. The red color of SO (3.6  $\text{mg L}^{-1}$ ) disappeared in the presence of 0.12  $\text{g L}^{-1}$  Ag- $\text{TiO}_2$  after 70 min under UV light, as observed by El-Kemary et al. [13]. However, 51% of dye was degraded in an illuminated ZnS nanophotocatalyst at neutral pH as mentioned in another study by El-Kemary et al. [11]. The modification of  $\text{TiO}_2$  structure, the synthesis of new catalysts or including oxidants to the photocatalytic systems have been adopted to improve performance. Earlier investigations have focused on the involvement of oxyhalogen anions for enhancing the photocatalytic treatment efficiency. The effect of oxyhalogens like  $\text{BrO}_3^-$ ,  $\text{ClO}_3^-$ ,  $\text{IO}_3^-$ ,  $\text{IO}_4^-$ , etc., as effective photoelectron quenchers has been assessed in many research papers. Choy et al. [14] included each of  $\text{BrO}_3^-$ ,  $\text{ClO}_3^-$  and  $\text{IO}_3^-$  for improving the photocatalytic destruction of *o*-chloroaniline in a UV/ $\text{TiO}_2$  system. Oxyhalogen processes were more efficient in the order  $\text{ClO}_3^- < \text{BrO}_3^- < \text{IO}_3^-$ , where an adequate amount of iodate could completely degrade *o*-chloroaniline within a minute, as reported by Choy et al. [14]. Similar findings were registered by Wu et al. [15] using periodate ( $\text{IO}_4^-$ ) to eliminate Reactive Red 198 dye in aqueous solution. Wang et al. [16] stated that  $\text{H}_2\text{O}_2$ ,  $\text{IO}_4^-$  and  $\text{S}_2\text{O}_8^{2-}$  had a pronounced rate-enhancing effect on the photocatalytic treatment of an aqueous solution of 2-chlorobiphenyl. Other investigations supported these results and confirmed the ability of the UV/ $\text{TiO}_2$ / $\text{IO}_4^-$  system to treat a large range of organics successfully [17–19].

Despite the important published works [17–19] on the UV/ $\text{TiO}_2$ / $\text{IO}_4^-$  system, the application of this emerging process for the treatment of textile dyes is rather limited. Additionally, although the enhancing effect of applying a UV/ $\text{TiO}_2$ / $\text{IO}_4^-$  system was usually reported to be noteworthy, very limited information is available on the influence of processing conditions on the technique efficiency. Moreover, the viability of the process in wastewater treatment depends on a TOC abatement evaluation. All these tasks have not been researched previously, probably due to the novelty of the process.

In the present work, the application of  $\text{TiO}_2$ -mediated photocatalysis in the presence of periodate ions (UV/ $\text{TiO}_2$ / $\text{IO}_4^-$ ) was examined for the treatment of an aqueous solution polluted with SO dye and compared with the UV/ $\text{TiO}_2$  classical system. The degradation efficiency was examined with various influencing factors such as initial dye concentration, catalyst loading, periodate concentration, liquid temperature, initial solution pH and dissolved gasses. The organic matter depletion was also monitored during the reaction, determined by the TOC analysis results.

## 2. Results and Discussion

### 2.1. Photocatalytic Degradation of SO

TiO<sub>2</sub>-mediated photocatalysis in the presence of periodate ions (IO<sub>4</sub><sup>−</sup>, 0.15 mM) was applied for the removal of SO (10 mg L<sup>−1</sup>) over illuminated TiO<sub>2</sub> (Degussa P25, 0.4 g L<sup>−1</sup>) at 25 °C and natural pH (~6). A series of experiments were first carried out under different systems, namely: (i) IO<sub>4</sub><sup>−</sup> only, (ii) UV/IO<sub>4</sub><sup>−</sup> and (iii) UV/TiO<sub>2</sub>. Results were reported in Figure 1, which represents the evolution of C/C<sub>0</sub> (C: concentration of SO at time t, C<sub>0</sub>: initial concentration of SO) as function of reaction time. The presence of periodate on its own or with the photocatalyst was found to be meaningless for dye removal; however, slight oxidation was observed under illuminated periodate, estimated to be 19% within 50 min, as shown Figure 1. The feeble effect of direct photolysis of periodate was expected due to the fact that periodate can produce •OH radicals and other reactive oxidants when it absorbs UV light at wavelengths of less than 300 nm [20].

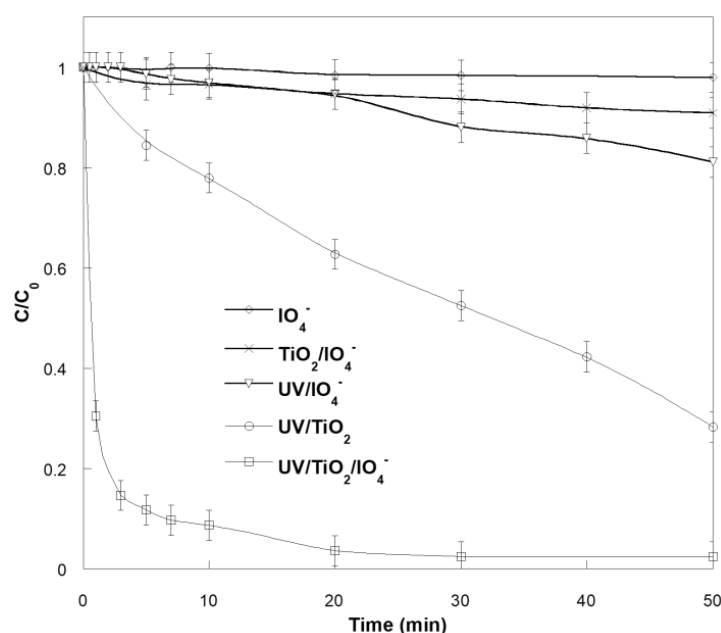
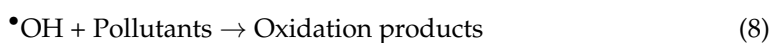


**Figure 1.** Degradation of SO in different systems (conditions: [IO<sub>4</sub><sup>−</sup>] = 0.15 mM, [TiO<sub>2</sub>] = 0.4 g L<sup>−1</sup>, [SO] = 10 mg L<sup>−1</sup>, T = 25 ± 2 °C, pH~6).

When a SO dye solution containing 0.4 g L<sup>−1</sup> of TiO<sub>2</sub> was exposed to UV light, the dye concentration reduced continuously with irradiation time, e.g., about 72% of the initial amounts were degraded after 50 min. These findings can be attributed to the photogeneration of holes,  $h^+$ , in the valence band and electrons,  $e^-$ , in the conduction band as oxidative and reductive entities, respectively, at the level of illuminated TiO<sub>2</sub> (Equation (1)). The photocatalytic oxidation of organics can proceed either directly, when the adsorbed substrate reacts with free and delocalized holes in the crystal lattice (Equation (7)), or by the means of free radicals (mainly •OH and O<sub>2</sub>•<sup>−</sup>) (Equation (8)) in the vicinity of TiO<sub>2</sub> particles or in the bulk solution, this is called indirect photocatalysis.



By the addition of a quantity of IO<sub>4</sub><sup>−</sup> (0.15 mM), the extent of removal increased substantially from 38% under UV/TiO<sub>2</sub> to 97% after just 20 min of irradiation time. This behavior can be explained by the fact that more reactive radicals (•OH, IO<sub>3</sub>• and IO<sub>4</sub>•) and non-radical species (O<sub>3</sub>, IO<sub>3</sub><sup>−</sup> and IO<sub>4</sub><sup>−</sup>) were produced in the UV/TiO<sub>2</sub>/IO<sub>4</sub><sup>−</sup> system. On the other hand, the presence of irreversible electron acceptors is a successful strategy to

avoid electron-hole recombination, which constitutes a major drawback in  $\text{TiO}_2$  mediated photocatalysis. As an effective electron acceptor, periodate increased the degradation rate by quenching surface electrons, hence, more oxidative reactions took place at holes level such as (Equations (2), (3) and (7)).

In several research works, photocatalytic kinetics were found to follow the Langmuir-Hinshelwood (L-H) model considering the substrate adsorption on the photocatalyst surface. Based on the following assumptions: (i) limited number of adsorption sites on the surface of photocatalyst, (ii) the site can adsorb only one molecule and the catalyst surface can be covered by monolayer, (iii) the adsorption reaction is reversible, (iv) the surface of catalyst is vigorously homogeneous and (v) there is no interaction between adsorbed molecules [21], the equation below was established:

$$\theta = \frac{Q_{ads}}{Q_{max}} = \frac{K_{ads} C}{1 + K_{ads} C} \quad (9)$$

where  $\theta$  is the  $\text{TiO}_2$  surface coverage,  $Q_{ads}$  is the adsorbed quantity,  $Q_{max}$  is the maximal adsorbed quantity,  $C$  is the concentration of the compound and  $K_{ads}$  is the Langmuir adsorption constant.

Since photocatalytic oxidation takes place not only between adsorbed molecules but also in aqueous solution, the modified L-H model (Equation (10)) was applied for a better fit to the process mechanism and for easily predicting the kinetic parameters.

$$r = -\frac{dC}{dt} = \frac{K_r K_{LH} C}{1 + K_r K_{LH} C} \quad (10)$$

where  $r$  is the substrate degradation rate,  $C$  is concentration,  $t$  is illumination time,  $K_r$  is the degradation rate constant and  $K_{LH}$  is the constant of adsorption of reactant on the  $\text{TiO}_2$  surface.

Equation (10) can be simplified to Equation (11) as the concentration of dye was a millimolar solution (0.0285 mM) in all experiments.

$$r = -\frac{dC}{dt} = K_{app} C \quad (11)$$

where  $K_{app} = K_{LH} K_r$ .

Experimental data were exploited to determine different characteristics of SO degradation under UV/ $\text{TiO}_2$  and UV/ $\text{TiO}_2/\text{IO}_4^-$  systems. The plot of  $\ln(C/C_0) = f(t)$  was found to be linear indicating first-order kinetics. The apparent rate constant ( $K_{app}$ ,  $\text{min}^{-1}$ ) was defined as the slope of the regression line, while initial rate ( $r_0$ ,  $\text{mg L}^{-1} \text{min}^{-1}$ ) was calculated using Equation (12):

$$r_0 = K_{app} C_0 \quad (12)$$

In terms of kinetics, photocatalysis involving periodate ions (UV/ $\text{TiO}_2/\text{IO}_4^-$ ) was much faster for SO destruction with  $r_0 = 12.07 \text{ mg L}^{-1} \text{min}^{-1}$  versus  $0.295 \text{ mg L}^{-1} \text{min}^{-1}$  for periodate-free photocatalysis (UV/ $\text{TiO}_2$ ). These results are in line with the existing studies reporting the effect of periodate ions on photocatalysis performance [17,18,22].

## 2.2. Effect of Initial SO Concentration

The substrate loading is a controlling parameter on photocatalysis performance. With the aim of investigating the effect of dye amount, SO photo-degradation runs were conducted using various initial dye concentrations of 5, 10, 20 and 40  $\text{mg L}^{-1}$ , employing Degussa P25 (0.4  $\text{g L}^{-1}$ ) as the sole photocatalyst, and in the presence of periodate ions (0.15 mM) (Figure 2). The obtained results show that regardless of periodate presence, the degradation percentage decreased with the increase in initial dye concentration. Within 30 min under illuminated  $\text{TiO}_2$ , 81.3% was successfully removed from the solution, the initial SO concentration of which was 5  $\text{mg L}^{-1}$ , whereas 46.9%, 14.8% and 12.1% was eliminated from 10, 20 and 40  $\text{mg L}^{-1}$  initial dye concentration solutions, respectively.

In aqueous periodate, the quantum yield calculated for each concentration was 100% for  $5 \text{ mg L}^{-1}$ , 98.1% for  $10 \text{ mg L}^{-1}$ , 83.9% for  $20 \text{ mg L}^{-1}$  and 44.4% for  $40 \text{ mg L}^{-1}$  after 30 min of reaction.

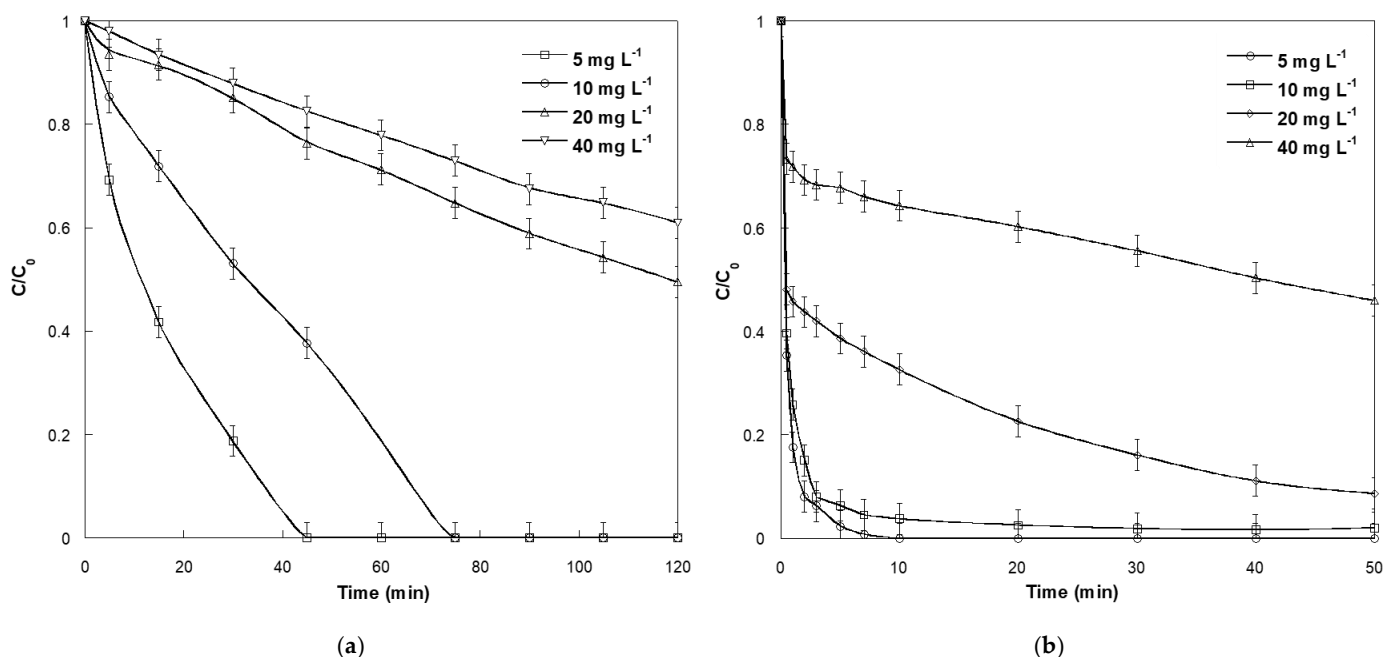


**Figure 2.** Effect of initial concentration of SO on its photocatalytic degradation by (a) conventional  $\text{TiO}_2$ -mediated photocatalysis and (b) in a UV/ $\text{TiO}_2$ /periodate system (conditions:  $0.4 \text{ g L}^{-1} \text{ TiO}_2$ , natural pH~6,  $T = 25 \pm 2^\circ\text{C}$ ,  $[\text{IO}_4^-] = 0.15 \text{ mM}$ ).

The dependence of degradation rate on the initial dye concentration was checked in the studied range and the corresponding findings are presented in Figure 3. It was noted that  $r_0$  lowered slightly from 0.3 to  $0.16 \text{ mg L}^{-1} \text{ min}^{-1}$  when SO initial concentration increased from 5 to  $40 \text{ mg L}^{-1}$  in periodate-free photocatalysis. The same findings were reported by Vulliet et al. [23] and Bekkouche et al. [24].

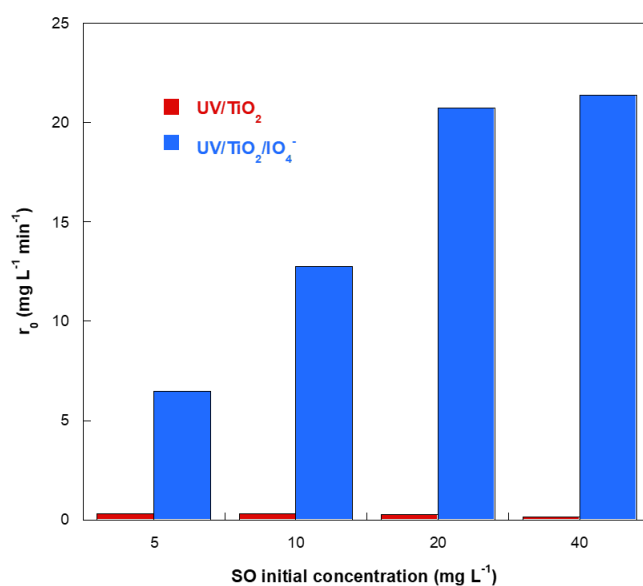


**Figure 3.** Dependence of initial degradation rate on SO concentration in the range of 5–40  $\text{mg L}^{-1}$  under UV/ $\text{TiO}_2$  and UV/ $\text{TiO}_2$ / $\text{IO}_4^-$  systems (conditions:  $0.4 \text{ g L}^{-1} \text{ TiO}_2$ , natural pH~6,  $T = 25 \pm 2^\circ\text{C}$ ,  $[\text{IO}_4^-] = 0.15 \text{ mM}$ ).

In contrast to conventional photocatalysis alone, the further increase in dye concentration led to an increase in the initial degradation rate in the presence of periodate. The  $r_0$  values were 6.46, 12.07, 20.75 and 21.37  $\text{mg L}^{-1} \text{min}^{-1}$  when  $C_0 = 5, 10, 20$  and  $40 \text{ mg L}^{-1}$ , respectively.

It should be pointed out that initial degradation rates for both systems (UV/TiO<sub>2</sub> and UV/TiO<sub>2</sub>/IO<sub>4</sub><sup>−</sup>) were determined a few minutes after the start of degradation from the curves showing  $C$  vs. time, instead of applying Equation (12). Even when the plots  $\ln(C/C_0)$  evolved linearly with time, the first-order rate constants did not remain constant when varying the initial concentration of the dye.

At higher SO concentrations, the majority of active sites were occupied on the photo-activated photocatalyst by adsorbed dye molecules, and the area around the TiO<sub>2</sub> became overcrowded. As a result, molecular water, oxygen and periodate could not easily reach the TiO<sub>2</sub> surface; hence, a smaller number of free radicals would be produced. In addition, under the same conditions of photocatalyst loading, light intensity and solution pH, the quantity of reactive species remains constant; consequently, the increase in SO initial concentration results in a reduction of degradation efficiency. In this case, SO decomposition was mainly promoted by direct photocatalysis.

### 2.3. Effect of TiO<sub>2</sub> Loading

Several researchers have reported that the key steps in the photocatalytic process occur on the semiconductor surface [25]. Accordingly, an examination of the effect of the active surface area = on photocatalytic degradation of SO dye under UV/TiO<sub>2</sub> and UV/TiO<sub>2</sub>/IO<sub>4</sub><sup>−</sup> systems was performed by using different amounts of TiO<sub>2</sub> in the range 0.01–3  $\text{g L}^{-1}$ , and by fixing the dye  $C_0$  (10  $\text{mg L}^{-1}$ ), periodate concentration (0.15 mM), temperature (25 °C) and pH of solution (~6). The normalized SO remaining concentration ( $C/C_0$ ) versus irradiation time was given in Figure 4a,b. As expected, the higher the semiconductor loading, the higher the degradation percentage was. For example, after 30 min of illumination, 80%, 60.4%, 56.3% and 40.4% of starting concentration were left in aqueous suspension with 0.01, 0.05, 0.1 and 0.4  $\text{g L}^{-1}$  TiO<sub>2</sub>, respectively. In the presence of IO<sub>4</sub><sup>−</sup>, it left only 32.9%, 6.2%, 2.3% and 1.9% from an initial dye solution of 10  $\text{mg L}^{-1}$  in the same order and conditions. Beyond 0.4  $\text{g L}^{-1}$ , a further increase in the semiconductor loading negatively affected the removal efficiency for both systems. This may be explained by the effect of light screening caused by accumulated particles of TiO<sub>2</sub>, which results in bad dispersion and penetration of light and subsequently a limited photocatalysis.

The dependence of the initial degradation rate of SO in catalyst loading was also studied (Figure 5). Similar trends were observed under both systems;  $r_0$  increased from 0.06 to 0.27  $\text{mg L}^{-1} \text{min}^{-1}$  in the UV/TiO<sub>2</sub> system, and from 1.08 to 7.41 in the UV/TiO<sub>2</sub>/IO<sub>4</sub><sup>−</sup> system when TiO<sub>2</sub> concentration increased from 0.01 to 0.4  $\text{g L}^{-1}$ . Kinetically, the increase in photocatalyst amount led to an enlargement in the illuminated surface, thus: (i) more conduction electrons and valence holes were generated, (ii) there were more adsorbed molecules and (iii) a high number of powerful oxidants was produced. Nevertheless, the initial rate dropped quickly to 0.19 and 6.28  $\text{mg L}^{-1} \text{min}^{-1}$  for 3  $\text{g L}^{-1}$  of irradiated TiO<sub>2</sub> in the absence and the presence of periodate, respectively. Hence, 0.4  $\text{g L}^{-1}$  was found to be the best concentration of TiO<sub>2</sub>. Similar results were observed by Zalazar et al. ([TiO<sub>2</sub>]<sub>opt</sub> = 0.5  $\text{g L}^{-1}$ ) [26], Torres et al. ([TiO<sub>2</sub>]<sub>opt</sub> = 1  $\text{g L}^{-1}$ ) [27] and Van Doorslaer et al. ([TiO<sub>2</sub>]<sub>opt</sub> = 5  $\text{g L}^{-1}$ ) [28]. The variation in optimum catalyst loading can be justified by the different reactor geometry as well as the conditions in which the degradation experiments were performed.



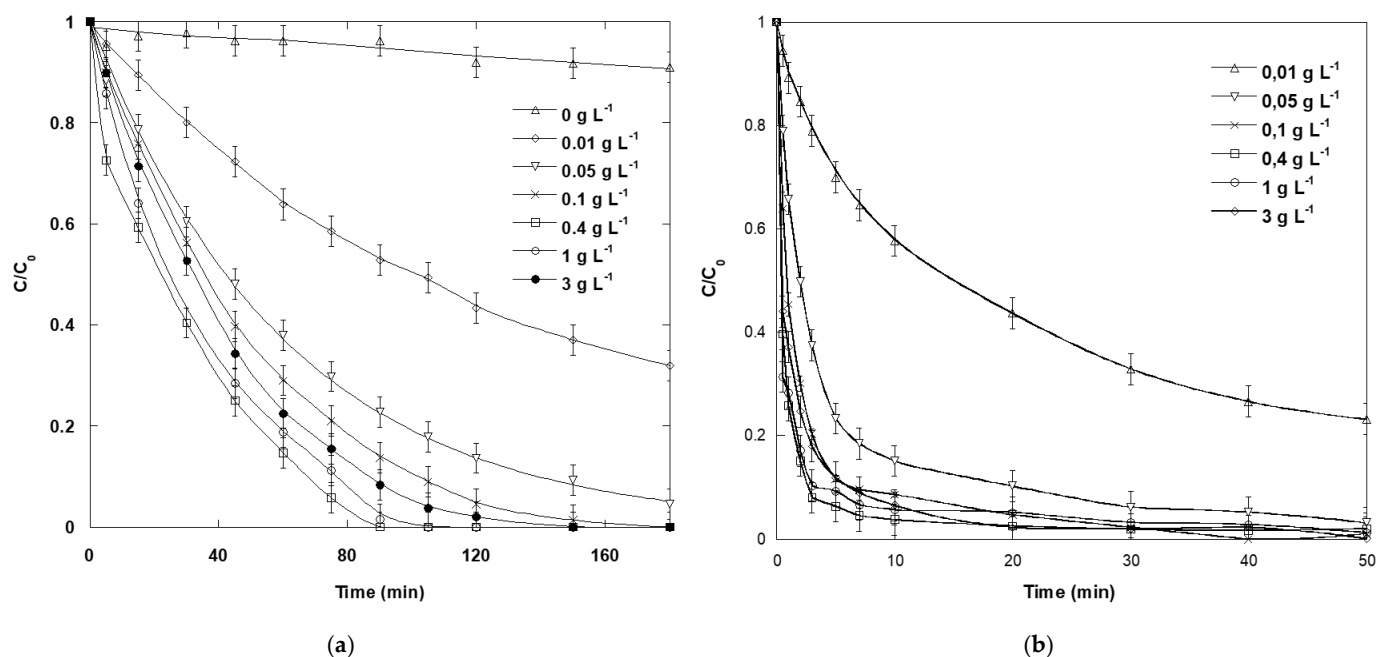


**Figure 4.** Effect of titanium dioxide concentration on SO degradation under (a) conventional photocatalysis and (b) photocatalysis in the presence of periodate (0.15 mM) (conditions:  $[\text{SO}] = 10 \text{ mg L}^{-1}$ , pH ~6,  $T = 25 \pm 2 \text{ }^\circ\text{C}$ ).

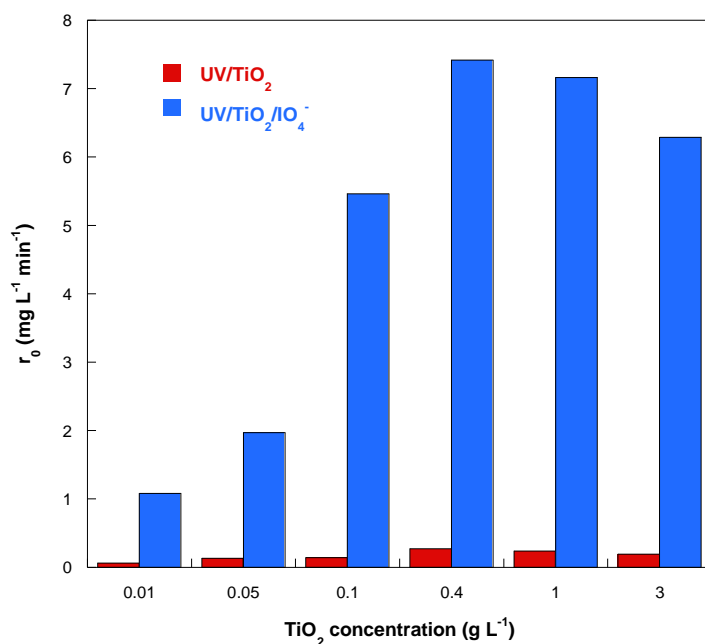


**Figure 5.** Initial degradation rate of SO ( $10 \text{ mg L}^{-1}$ ) as function of photocatalyst loading (0, 0.01, 0.05, 0.1, 0.4, 1 and 3 g L<sup>-1</sup>) at pH~6 and  $T = 25 \pm 2 \text{ }^\circ\text{C}$ .

#### 2.4. Effect of Periodate Concentration

Figure 6a depicts the effect of  $\text{IO}_4^-$  dosage over the range of 0.01–1 mM on the removal efficiency of SO ( $10 \text{ mg L}^{-1}$ ) after 15 min in the UV/ $\text{TiO}_2/\text{IO}_4^-$  system. Corresponding trials were carried out in an aqueous suspension of  $0.4 \text{ g L}^{-1}$  photocatalyst at  $25 \text{ }^\circ\text{C}$  and natural pH (~6). According to Figure 6a, the increase in periodate concentration caused a continuous rise in the photocatalytic degradation efficiency by 50.4% with increasing  $[\text{IO}_4^-]_0$  from 0.01 to 0.08 mM, 14.1% with an increase from 0.08 to 0.15 mM and 2.2% with an increase from 0.15 to 0.2 mM. Up to 0.2 mM of  $\text{IO}_4^-$ , the dye degradation was deemed

complete; thus, the removal percent remained constant (100%) regardless of the amount of periodate added. The presence of more periodate anions (i) progressively increased the amount of produced reactive oxygen species (ROS), especially  $\bullet\text{OH}$ ,  $\text{O}_2^{\bullet-}$  and  $\text{IO}_3^\bullet$  (Equations (13)–(19) [29]), (ii) trapped more ejected electrons from illuminated titanium dioxide, resulting in deferring rapid  $e^-/h^+$  recombination, and (iii) made more holes available for more oxidation reactions.

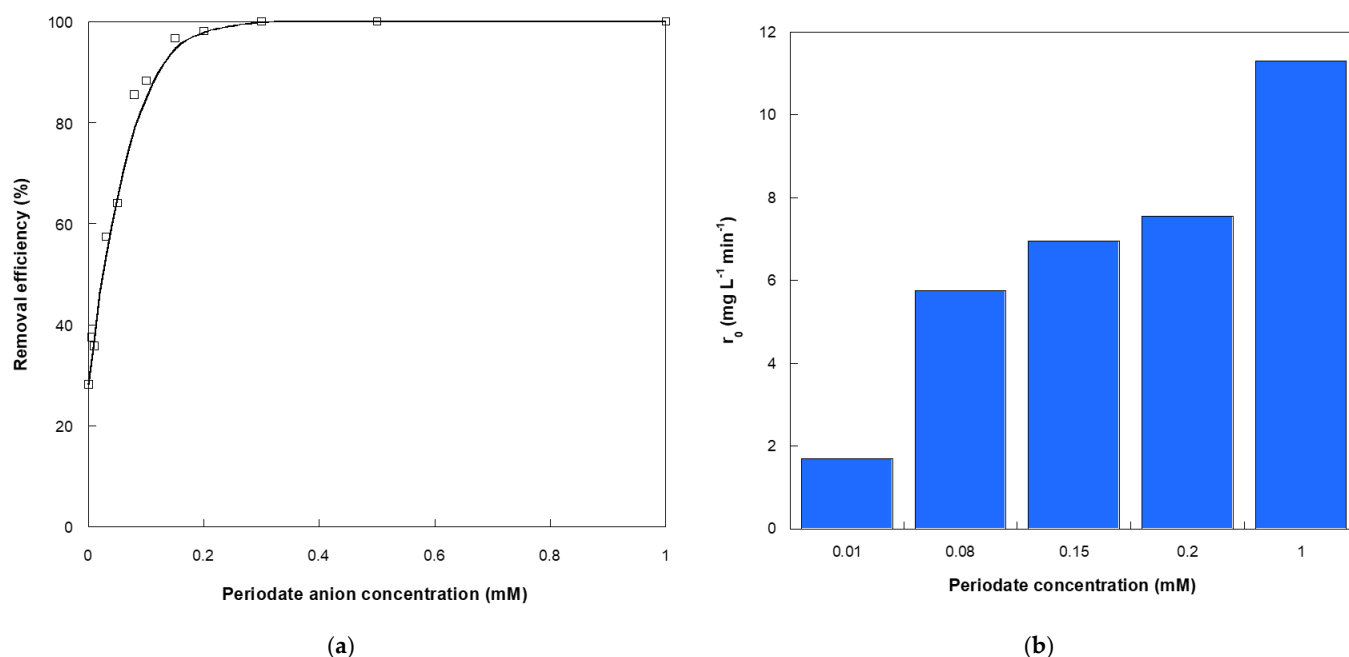
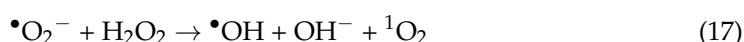
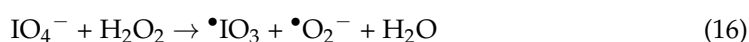
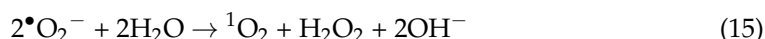
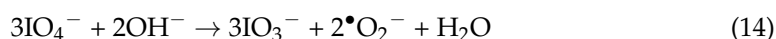
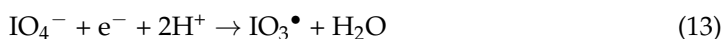


**Figure 6.** Effect of periodate concentration on (a) removal efficiency of SO within 15 min of illumination and (b) initial degradation rate of SO (conditions:  $[\text{TiO}_2] = 0.4 \text{ g L}^{-1}$ ,  $[\text{SO}] = 10 \text{ mg L}^{-1}$ ,  $T = 25 \pm 2^\circ\text{C}$ ,  $\text{pH} \sim 6$ ).

On the other hand, the kinetic investigations revealed a proportional enhancement of the initial degradation rate of SO as a function of periodate concentration in the studied interval (Figure 6b). The initial degradation rate increased from  $1.64$  to  $11.32 \text{ mg L}^{-1} \text{ min}^{-1}$  when the periodate dosage varied from  $0.01$  to  $1 \text{ mM}$ , and no overdose effect was observed. This statement is in excellent agreement with previous studies such as those by Yun et al. [19] using visible-light/ $\text{TiO}_2/\text{IO}_4^-$  ( $0$ – $1 \text{ mM}$ ), Sadik et al. [17] employing  $\text{UV}_{254}/\text{TiO}_2/\text{IO}_4^-$  ( $0.0476$ – $1 \text{ mM}$ ) and Gözmen et al. [3] adopting  $\text{UV}_{365}/\text{TiO}_2/\text{IO}_4^-$  ( $1$ – $10 \text{ mM}$ ). However, a negative effect was noted in the presence of excess periodate up to a threshold found to be  $3 \text{ mM}$  under photoactivated periodate system as reported Wu et al. [15], while Lee et al. [20] and Chadi et al. [30] observed a decrease in the degradation rate beyond  $5 \text{ mM}$  of activated periodate by  $\text{UV}_{254}$  or  $\text{H}_2\text{O}_2$ , respectively. These findings were justified by the fact that periodate at higher concentrations acted as a free



radical scavenger, resulting in limited reactivity. It is clear that the presence of  $\text{TiO}_2$  ruled out the scavenger effect of excess periodate, hence improving the process effectiveness.

### 2.5. Effect of the Liquid Temperature

The temperature of reactional liquid plays an important role in chemical reactions. In the case of heterogeneous photocatalysis, the adsorption/desorption of reagents onto the catalyst, as well as the dissolution of oxygen depend strongly on solution temperature [31,32]. In order to examine the temperature effect on the performance of UV/ $\text{TiO}_2$  and UV/ $\text{TiO}_2/\text{IO}_4^-$  systems to remove SO dye ( $10 \text{ mg L}^{-1}$ ) from water, tests were conducted at four temperatures (15, 25, 35 and  $45^\circ\text{C}$ ) employing  $0.15 \text{ mM}$  of periodate and  $0.4 \text{ g L}^{-1}$  of  $\text{TiO}_2$  at natural solution pH. The dependence of initial degradation rate ( $r_0$ ) on temperature is illustrated in Figure 7. A slight increase in the degradation rate was observed over the tested range ( $15\text{--}45^\circ\text{C}$ ) both in UV/ $\text{TiO}_2$  and UV/ $\text{TiO}_2/\text{IO}_4^-$  systems. This was estimated to be by  $0.067 \text{ mg L}^{-1} \text{ min}^{-1}$  in the conventional system versus  $1.22 \text{ mg L}^{-1} \text{ min}^{-1}$  in the presence of periodate when increasing from 15 to  $45^\circ\text{C}$ . These findings are supported by Yawalkar et al. [33], Bhatkhande et al. [34] and Fox et al. [35]. Yawalkar et al. [33] found a small effect of temperature ( $38\text{--}75^\circ\text{C}$ ) on the photocatalytic degradation of phenol under solar light. They reported that the reaction rate was found to be almost constant ( $0.376 \text{ mg L}^{-1} \text{ min}^{-1}$ ) at a solar intensity of  $63 \text{ mW}$ , regardless of the liquid temperature. Bhatkhande et al. [34] and Fox et al. [35] stated that the process was weakly dependent on minor variations in temperature. The effect of heating on periodate-assisted photocatalysis has not been assessed previously. In contrast to the degradation in the presence of periodate, the photocatalytic degradation of SO in the presence of persulfate was found to be highly sensitive to a temperature rise over the range of  $25\text{--}70^\circ\text{C}$ , as reported by Bekkouche et al. [24]. They attributed these results to the thermal activation of persulfate in the studied interval, resulting to increased reactivity.

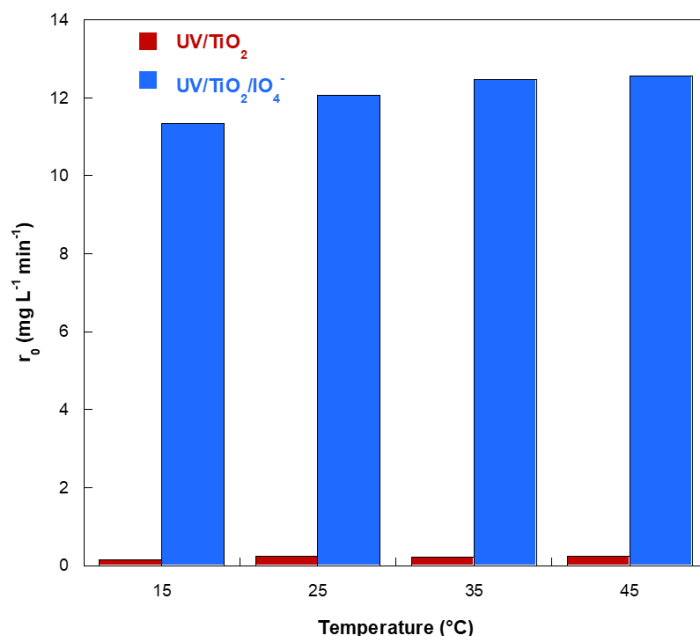


**Figure 7.** Dependence of initial rate of photocatalytic degradation of SO ( $10 \text{ mg L}^{-1}$ ) on solution temperature varying in the range  $15\text{--}45^\circ\text{C}$  (conditions:  $[\text{TiO}_2] = 0.4 \text{ g L}^{-1}$ ,  $\text{pH} \sim 6$ ).

### 2.6. Effect of Initial Solution pH

The effect of the initial pH of the media on heterogeneous photocatalysis has been the subject of many studies [19,36–39], since its variation can affect the characteristics of both the photocatalyst and pollutant. The influence of initial solution pH on the effectiveness of SO removal by photocatalytic treatment in the absence and presence of periodate ( $0.15 \text{ mM}$ )

was also investigated. It should be pointed out that SO was stable regardless of the solution pH. Figure 8 shows the SO removal yield–pH profiles within 5 min in the UV/TiO<sub>2</sub> and UV/TiO<sub>2</sub>/IO<sub>4</sub><sup>−</sup> systems, varying the initial solution pH in the range of 2–12. Both systems presented the same behavior but with more efficiency in the presence of periodate, e.g., the periodate system was nine times more efficient than the conventional photocatalysis system in dye degradation at pH of 2 after 5 min of reaction. The removal yield augmented significantly with increasing the initial pH from 2 to 10 as the result of the increased production of free radicals. After 5 min in the UV/TiO<sub>2</sub>/IO<sub>4</sub><sup>−</sup> system, 74.6% was efficiently eliminated at pH 2, 79.7% at pH 4, 93.7% at pH 6, 94.9% at pH 8 and 97.8% at pH 10, compared to 38.7%, 43.5%, 47.5%, 57.0% and 84.7% in periodate-free solution for the same duration and pH order.

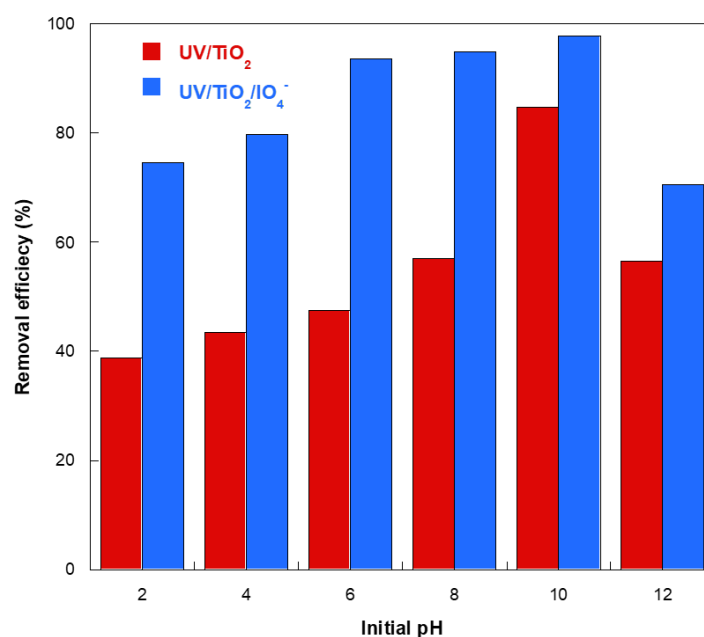


**Figure 8.** Effect of initial solution pH on removal efficiency of SO (10 mg L<sup>−1</sup>) within 5 min under UV/TiO<sub>2</sub> and UV/TiO<sub>2</sub>/IO<sub>4</sub><sup>−</sup> systems (conditions: [IO<sub>4</sub><sup>−</sup>] = 0.15 mM, [TiO<sub>2</sub>] = 0.4 g L<sup>−1</sup>, T = 25 ± 2 °C).

Between pH 1 and 8, the predominant periodate species was IO<sub>4</sub><sup>−</sup>, and at pH 10, it was H<sub>2</sub>I<sub>2</sub>O<sub>10</sub><sup>4−</sup>. The deprotonated and the dimerized (H<sub>2</sub>I<sub>2</sub>O<sub>10</sub><sup>4−</sup>) species of periodate are both reactive in the photo-decomposition of organic pollutants [20]. Based on this data, the enhancement of degradation efficiency in alkaline media might be explained by other factors, mainly the change in the charge of the semiconductor surface (the dye is cationic regardless of solution acidity). The p*H*<sub>zpc</sub> is described as the pH value at which the net charge of the semiconductor surface is equal to zero. If pH < p*H*<sub>zpc</sub> (6.8, TiO<sub>2</sub> Degussa P25), the photocatalyst surface is negatively charged (Equation (20)), and if pH is more than p*H*<sub>zpc</sub>, its charge is positive (Equation (21)).



In alkaline media (pH > p*H*<sub>zpc</sub>), a strong adsorption of the dye onto the catalyst is more favorable due to the electrostatic attraction between the negatively charged TiO<sub>2</sub> and the dye. Consequently, the photo-degradation efficiency is enhanced. At pH < 6, coulombic repulsion takes place, thus the dye molecules are scarcely adsorbed and therefore a negative effect of pH on the photocatalytic process is clearly observed. The high concentration of

hydroxyl anions ( $^-\text{OH}$ ) at higher pH is an important source of hydroxyl radicals ( $^{\bullet}\text{OH}$ ), which can effectively oxidize the dye molecules.

At pH 12, the degradation extent was remarkably decreased for each system. The percentage of dye removal was reduced by 28.3% and 27.3% during 5 min in the UV/TiO<sub>2</sub> and UV/TiO<sub>2</sub>/IO<sub>4</sub><sup>−</sup> systems, respectively, moving from pH 10 to 12. These results may be explained by the agglomeration of TiO<sub>2</sub> particles at higher pH. On the other hand, the scavenging of free radicals by carbonate anions that might be produced from CO<sub>2</sub> as a mineralization product of SO is expected at pH > 10.33 [30]. In our experimental conditions (results not shown), the influence of carbonate anions at lower concentration revealed a negative effect on the photocatalytic decay of SO under both systems. The carbonate anions can react with  $^{\bullet}\text{OH}$  and O<sub>2</sub> $^{\bullet-}$  to produce carbonate radicals (CO<sub>3</sub> $^{\bullet-}$ ) which causes a loss in efficiency in dye degradation.

The pH variations affect the concentration of reactive species yielded during the photocatalysis processes, which directly affects their performance toward SO removal.

### 2.7. Effect of Dissolved Gases

In order to determine the role of dissolved oxygen in photocatalytic oxidation of SO, the saturation by air (21% O<sub>2</sub>) followed by oxygen-free gases (N<sub>2</sub> and Ar) was conducted in the absence and presence of periodate (0.15 mM). The gases were continuously bubbled through the solution for 15 min in the dark and also during illumination time using an immersed sparger. The results for each system are given in Figure 9. In the conventional photocatalysis (Figure 9a), the degradation was slightly improved in the presence of more dissolved oxygen provided by aeration, by approximatively only 5% compared with the unsaturated system. In addition to the generation of powerful free radicals (O<sub>2</sub> $^{\bullet-}$  and H<sub>2</sub>O<sub>2</sub>), the oxygen molecule can act as a scavenger of photo-generated electrons which can defer the hole-electron pair recombination, thus freeing up holes for more reactions [40,41]. However unlikely, the weak solubility of oxygen and its limited adsorption on the semiconductor surface can also be a rate limiting factor in the photocatalytic decomposition of organic pollutants in high concentration or at low level of dissolved oxygen, as reported Gerischer et al. [42].

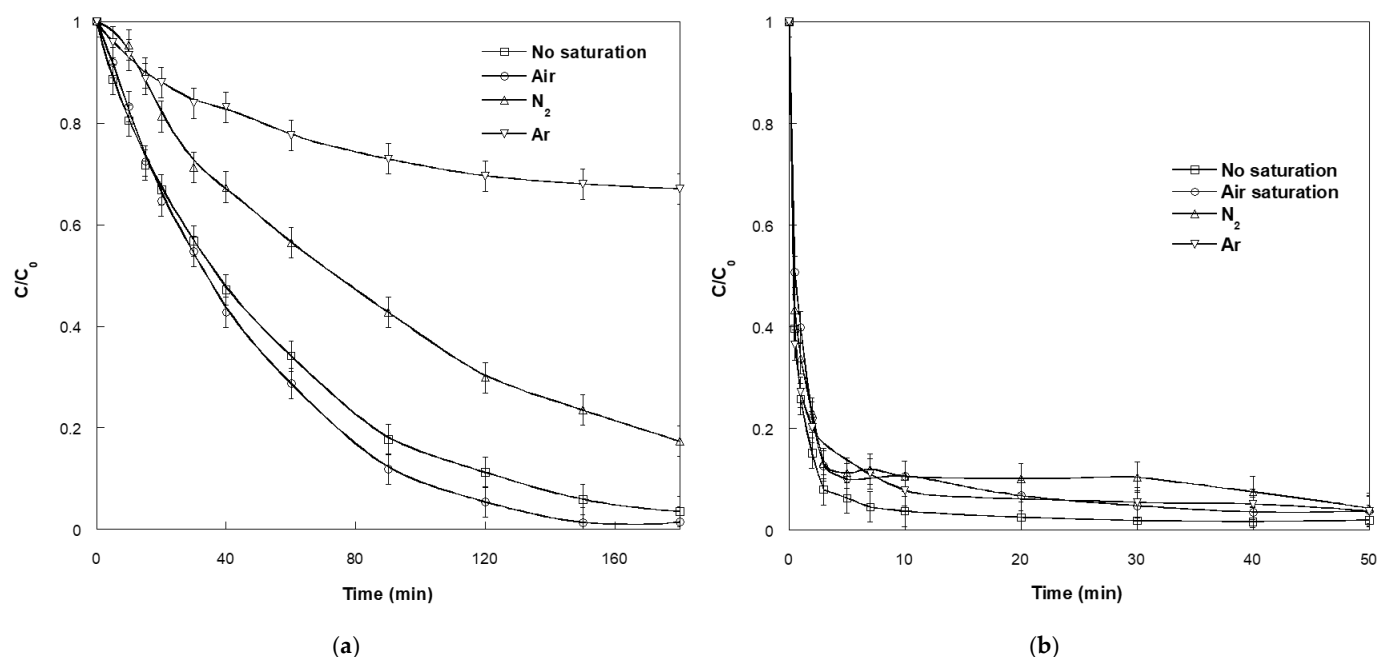


**Figure 9.** Effect of dissolved gases on photocatalytic degradation of SO (10 mg L<sup>−1</sup>) in: (a) UV/TiO<sub>2</sub> and (b) UV/TiO<sub>2</sub>/IO<sub>4</sub><sup>−</sup> systems (conditions: [TiO<sub>2</sub>] = 0.4 g L<sup>−1</sup>, [IO<sub>4</sub><sup>−</sup>] = 0.15 mM, T = 25 ± 2 °C and pH~6).

Under  $N_2$  and Ar sparging, the removal of the target compound became very slow in the order of  $Ar < N_2$ . These results agree with many reported studies [43,44]. The incomplete inhibition under oxygen-free conditions may confirm that oxygen is not the sole source of reactive radicals. Moonsiri et al. [40] found limited dissolved oxygen reduced the concentration of degradation intermediates as well as their types; hence, an alternative degradation pathway was probably followed.

In the presence of 0.15 mM periodate (Figure 9b), a slight inhibition was registered under either aeration or zero-oxygen conditions (Ar and  $N_2$ ). The competitive reactions between  $IO_4^-$  and the adsorbed oxygen to quench the conduction band electrons may be responsible for the degradation slow-down during aeration. Moreover, the effectiveness of this system seemed to be less sensitive to the zero-oxygen medium. Periodate as an electron acceptor played practically the same role of oxygen.

## 2.8. Mineralization

The efficiency of the photocatalytic systems were evaluated by monitoring the decolorization during reaction time, i.e., the destruction of the chromosphere group responsible for the dye color. However, the mineralization means that the conversion of hole organic matter, including the parent molecule and its degradation products, usually leads to  $CO_2$ ,  $H_2O$  and mineral compounds. Sometimes, the degradation products are more toxic than the starting molecule. In this case, a complete mineralization of organic pollutants would be required.

The mineralization of SO in the  $UV/TiO_2/IO_4^-$  and  $UV/TiO_2$  systems was examined ( $10\text{ mg L}^{-1}$  SO,  $0.4\text{ g L}^{-1}$   $TiO_2$ ,  $0.15\text{ mM}$   $IO_4^-$ ,  $25\text{ }^\circ\text{C}$  and natural pH) using TOC (Total Organic Carbon) analysis. The depletion of TOC concentration as a function of reaction time is depicted in Figure 10. Despite the rapid decolorization in the periodate system, approximately equal TOC removal efficiency was obtained for both systems. In the presence of periodate, the complete decolorization was achieved in 50 min, while just 30% of dye concentration was mineralized in this duration. In illuminated  $TiO_2$ , a discolored solution was obtained after 3 h of reaction in which 62% was converted to minerals. These outcomes are in harmony with other studies. Ohtaki et al. [45] observed a strong inhibition of coexisting halide ions against complete mineralization of the surfactants by photocatalytic process in the order:  $I^- > Br^- \gg Cl^-$ . The production of iodide ( $I^-$ ) during the periodate system can be an explanation for limited mineralization.

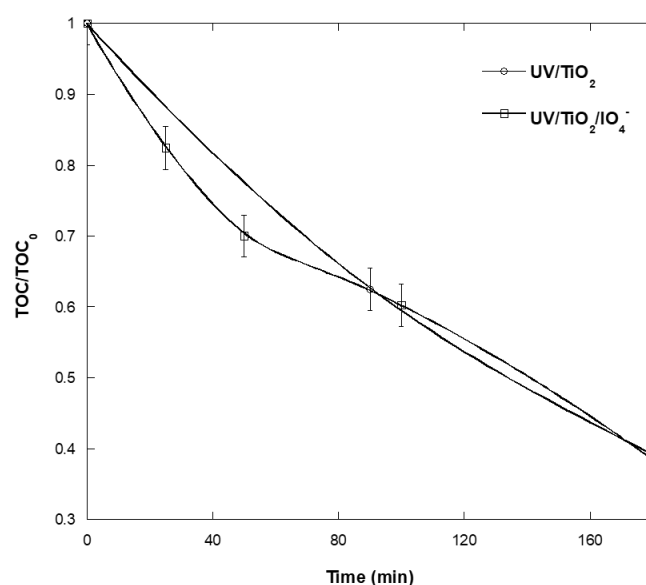


**Figure 10.** Mineralization during photocatalytic degradation of SO ( $10\text{ mg L}^{-1}$ ) in conventional photocatalysis ( $UV/TiO_2$ ) and periodate system ( $UV/TiO_2/IO_4^-$ ) (conditions:  $[TiO_2] = 0.4\text{ g L}^{-1}$ ,  $[IO_4^-] = 0.15\text{ mM}$ ,  $T = 25 \pm 2\text{ }^\circ\text{C}$  and  $pH \sim 6$ ).

### 3. Materials and Methods

#### 3.1. Reagents

SO and sodium periodate ( $\text{NaIO}_4$ ) were provided by Fluka and Sigma-Aldrich, respectively. For pH adjustment,  $\text{NaOH}$  and  $\text{H}_2\text{SO}_4$  were purchased from Sigma-Aldrich. The photocatalyst used in this study was  $\text{TiO}_2$  Degussa P25 (80% anatase and 20% rutile, average particle size: 30 nm, specific surface area:  $50 \text{ m}^2 \text{ g}^{-1}$ ), which was supplied by Evonik. All stock solutions were prepared with deionized water and all reagents were used without further purification. Deionized water was utilized to prepare all solutions, and ultra-pure water for TOC analysis.

#### 3.2. Photocatalysis Experiments and Apparatus

The photocatalytic experiments were conducted in a cylindrical water jacketed Pyrex reactor with a capacity of 500 mL, equipped with a magnetic stirring bar. The light irradiation was provided by a low-pressure mercury lamp ( $15 \text{ mW cm}^{-2}$ , Oriel 6035) emitting mainly at 365 nm, placed in a quartz tube. The lamp was totally immersed in the solution and fixed vertically at the center of the reactor at about 3 cm from the bottom.

The mixture of 200 mL SO solution ( $10 \text{ mg L}^{-1}$ ) and a quantity of  $\text{TiO}_2$  ( $0.4 \text{ g L}^{-1}$ ) was first agitated at  $25 \pm 2^\circ\text{C}$  for 30 min in the dark to ensure the complete adsorption/desorption equilibrium of the pollutant. For the conventional system, the lamp was turned on just after this period. Concerning the UV/ $\text{TiO}_2/\text{IO}_4^-$  system experiments, a sufficient amount of  $\text{NaIO}_4$  was added to the reactional liquid simultaneously with the lamp illumination. After centrifugation (10,000 rpm during 30 min), the aliquots taken at different time intervals were analyzed at 519 nm using a UV-Visible spectrophotometer (Biochrom, Holliston, MA, USA) equipped with quartz cuvettes of 1 cm light path. Sufficient amounts of  $\text{H}_2\text{SO}_4$  or  $\text{NaOH}$  were added to the SO solution in order to adjust its pH.

It is important to note that the variation in SO solution pH in the range of 1–10 affected neither  $\lambda_{\text{max}}$  nor the initial absorbance at  $\lambda_{\text{max}}$ .

The mineralization of SO solutions was monitored by measuring the total organic carbon (TOC) content in different centrifuged samples using a MembraPure UniTOC-lab analyzer. The instrument, equipped with an automatic sample injector, uses UV/persulfate oxidation followed by  $\text{CO}_2$  selective highly sensitive non-dispersive infrared detection.

All trials were carried out in triplicate and the mean values were reported.

### 4. Conclusions

The treatment of an aqueous solution of SO solely with  $\text{TiO}_2$ -mediated photocatalysis (UV/ $\text{TiO}_2$ ) and then in the presence of periodate anion revealed a higher performance in the UV/ $\text{TiO}_2/\text{IO}_4^-$  system. It was found that the degradation efficiency increased with an increase in periodate concentration with no overdose pH variation effect. The removal of SO was also examined for different initial dye concentrations and photocatalyst amounts. The dye destruction was more efficient at low initial SO concentration, while  $0.4 \text{ g L}^{-1}$  was found to be the best concentration for  $\text{TiO}_2$ . Both photocatalytic systems presented a strong dependence on initial solution pH where the degradation rates increased proportionally with pH value up to a pH of 10 and decreased afterward. However, the performance of all systems seemed insensitive to the liquid temperature changes. The role of dissolved gases on decay yield was tested in the presence of air, nitrogen and argon atmospheres. A negative effect was observed under nitrogen and argon conditions for the UV/ $\text{TiO}_2$  system. At higher dissolved oxygen levels, the degradation was clearly hampered in the UV/ $\text{TiO}_2/\text{IO}_4^-$  system, whereas a slight increase was observed in the absence of periodate. The TOC analysis revealed nearly the same abatement efficiency for target molecule mineralization in both systems (UV/ $\text{TiO}_2$  and UV/ $\text{TiO}_2/\text{IO}_4^-$ ). Finally, the residual amount of  $\text{IO}_4^-$  and the possible formation of iodine products may limit practical application of the UV/ $\text{TiO}_2/\text{IO}_4^-$  technique in water treatment. So far, there are no legislated discharge requirements for iodine compounds, but their intrinsic toxicity may

eventually lead to a restriction in permissible levels for all iodine species. Nevertheless, the process appears very promising as long as the involvement of  $\text{IO}_4^-$  is not very problematic.

**Author Contributions:** M.B.: Investigation, visualization, writing—original draft preparation and writing—review & editing; O.H.: supervision, conceptualization, methodology, formal analysis, project administration, resources, funding acquisition, investigation, validation and writing—review and editing; H.F.: validation, methodology, resources and writing—review and editing; A.A.: validation, visualization and writing—review and editing. All authors have read and agreed to the published version of the manuscript.

**Funding:** This research received no external funding.

**Data Availability Statement:** Not applicable.

**Acknowledgments:** The authors extend their appreciation to the Deputyship for Research & Innovation, Ministry of Education in Saudi Arabia for funding this research work through the project no. (IFKSURG-2-579).

**Conflicts of Interest:** The authors declare no conflict of interest.

## References

1. Pawar, R.C.; Lee, C.S. *Heterogeneous Nanocomposite-Photocatalysis for Water Purification*; William Andrew: Norwich, NY, USA, 2015; ISBN 9780323393133.
2. Zeghioud, H.; Assadi, A.A.; Khellaf, N.; Djelal, H.; Amrane, A.; Rtimi, S. Reactive species monitoring and their contribution for removal of textile effluent with photocatalysis under UV and visible lights: Dynamics and mechanism. *J. Photochem. Photobiol. A Chem.* **2018**, *365*, 94–102. [\[CrossRef\]](#)
3. Azzaz, A.A.; Assadi, A.A.; Jellali, S.; Bouzaza, A.; Wolbert, D.; Rtimi, S.; Bousselmi, L. Discoloration of simulated textile effluent in continuous photoreactor using immobilized titanium dioxide: Effect of zinc and sodium chloride. *J. Photochem. Photobiol. A Chem.* **2018**, *358*, 111–120. [\[CrossRef\]](#)
4. Ogugbue, C.J.; Sawidis, T. Bioremediation and Detoxification of Synthetic Wastewater Containing Triarylmethane Dyes by *Aeromonas hydrophila* Isolated from Industrial Effluent. *Biotechnol. Res. Int.* **2011**, *2011*, 967925. [\[CrossRef\]](#) [\[PubMed\]](#)
5. Malekbala, M.R.; Soltani, S.M.; Yazdi, S.K.; Hosseini, S. Equilibrium and Kinetic Studies of Safranin Adsorption on Alkali-Treated Mango Seed Integuments. *Int. J. Chem. Eng. Appl.* **2012**, *3*, 160–166.
6. Merouani, S.; Hamdaoui, O.; Bouhelassa, M. Degradation of Safranin O by thermally activated persulfate in the presence of mineral and organic additives: Impact of environmental matrices. *Desalin. Water Treat.* **2017**, *75*, 202–212. [\[CrossRef\]](#)
7. Sieren, B.; Baker, J.; Wang, X.; Rozzoni, S.J.; Carlson, K.; McBain, A.; Kerstan, D.; Allen, L.; Liao, L.; Li, Z. Sorptive Removal of Color Dye Safranin O by Fibrous Clay Minerals and Zeolites. *Adv. Mater. Sci. Eng.* **2020**, *2020*, 8845366. [\[CrossRef\]](#)
8. Hayat, K.; Gondal, M.A.; Khaled, M.M.; Yamani, Z.H.; Ahmed, S. Laser induced photocatalytic degradation of hazardous dye (Safranin-O) using self synthesized nanocrystalline WO<sub>3</sub>. *J. Hazard. Mater.* **2011**, *186*, 1226–1233. [\[CrossRef\]](#)
9. Gupta, V.K.; Jain, R.; Mittal, A.; Mathur, M.; Sikarwar, S. Photochemical degradation of the hazardous dye Safranin-T using TiO<sub>2</sub> catalyst. *J. Colloid Interface Sci.* **2007**, *309*, 464–469. [\[CrossRef\]](#)
10. Ekka, B.; Sahu, M.K.; Patel, R.K.; Dash, P. Titania coated silica nanocomposite prepared via encapsulation method for the degradation of Safranin-O dye from aqueous solution: Optimization using statistical design. *Water Resour. Ind.* **2019**, *22*, 100071. [\[CrossRef\]](#)
11. El-kemary, M.; El-shamy, H. Fluorescence modulation and photodegradation characteristics of safranin O dye in the presence of ZnS nanoparticles. *J. Photochem. Photobiol. A Chem.* **2009**, *205*, 151–155. [\[CrossRef\]](#)
12. Abdullah, F.H.; Rauf, M.A.; Ashraf, S.S. Photolytic oxidation of Safranin-O with H<sub>2</sub>O<sub>2</sub>. *Dye. Pigment.* **2007**, *72*, 2–5. [\[CrossRef\]](#)
13. El-kemary, M.; Abdel-moneam, Y.; Madkour, M.; El-mehasseb, I. Enhanced photocatalytic degradation of Safranin-O by heterogeneous nanoparticles for environmental applications. *J. Lumin.* **2011**, *131*, 570–576. [\[CrossRef\]](#)
14. Choy, W.K.; Chu, W. The use of oxyhalogen in photocatalytic reaction to remove o-chloroaniline in TiO<sub>2</sub> dispersion. *Chemosphere* **2007**, *66*, 2106–2113. [\[CrossRef\]](#) [\[PubMed\]](#)
15. Wu, M.-C.; Wu, C.-H. Decolorization of C.I. reactive red 198 in UV/oxidant and UV/TiO<sub>2</sub>/oxidant systems. *React. Kinet. Mech. Catal.* **2011**, *104*, 281–290. [\[CrossRef\]](#)
16. Wang, Y.; Hong, C.S. Effect of hydrogen peroxide, periodate and persulfate on photocatalysis of 2-chlorobiphenyl in aqueous TiO<sub>2</sub> suspensions. *Water Res.* **1999**, *33*, 2031–2036. [\[CrossRef\]](#)
17. Sadik, W.A. Effect of inorganic oxidants in photodecolourization of an azo dye. *J. Photochem. Photobiol. A Chem.* **2007**, *191*, 132–137. [\[CrossRef\]](#)
18. Gözmen, B.; Turabik, M.; Hesenov, A. Photocatalytic degradation of Basic Red 46 and Basic Yellow 28 in single and binary mixture by UV/TiO<sub>2</sub>/periodate system. *J. Hazard. Mater.* **2009**, *164*, 1487–1495. [\[CrossRef\]](#)



19. Yun, E.T.; Yoo, H.Y.; Kim, W.; Kim, H.E.; Kang, G.; Lee, H.; Lee, S.; Park, T.; Lee, C.; Kim, J.H.; et al. Visible-light-induced activation of periodate that mimics dye-sensitization of TiO<sub>2</sub>: Simultaneous decolorization of dyes and production of oxidizing radicals. *Appl. Catal. B Environ.* **2017**, *203*, 475–484. [\[CrossRef\]](#)
20. Lee, C.; Yoon, J. Application of photoactivated periodate to the decolorization of reactive dye: Reaction parameters and mechanism. *J. Photochem. Photobiol. A Chem.* **2004**, *165*, 35–41. [\[CrossRef\]](#)
21. Guettaï, N.; Amar, H.A. Photocatalytic oxidation of methyl orange in presence of titanium dioxide in aqueous suspension. Part II: Kinetics study. *Desalination* **2005**, *185*, 439–448. [\[CrossRef\]](#)
22. Chia, L. Kinetics and Mechanism of Photoactivated Periodate Reaction with 4-Chlorophenol in Acidic Solution. *Environ. Sci. Technol.* **2004**, *38*, 6875–6880. [\[CrossRef\]](#) [\[PubMed\]](#)
23. Vulliet, E.; Chovelon, J.; Guillard, C.; Herrmann, J. Factors influencing the photocatalytic degradation of sulfonylurea herbicides by TiO<sub>2</sub> aqueous suspension. *J. Photochem. Photobiol. A Chem.* **2003**, *159*, 71–79. [\[CrossRef\]](#)
24. Bekkouche, S.; Merouani, S.; Hamdaoui, O.; Bouhelassa, M. Efficient photocatalytic degradation of Safranin O by integrating solar-UV/TiO<sub>2</sub>/persulfate treatment: Implication of sulfate radical in the oxidation process and effect of various water matrix components. *J. Photochem. Photobiol. A Chem.* **2017**, *345*, 80–91. [\[CrossRef\]](#)
25. Minero, C.; Catozzo, F.; Pelizzetti, E. Role of adsorption in photocatalyzed reactions of organic molecules in aqueous titania suspensions. *Langmuir* **1992**, *8*, 481–486. [\[CrossRef\]](#)
26. Zalazar, C.S.; Martin, C.A.; Cassano, A.E. Photocatalytic intrinsic reaction kinetics. II: Effects of oxygen concentration on the kinetics of the photocatalytic degradation of dichloroacetic acid. *Chem. Eng. Sci.* **2005**, *60*, 4311–4322. [\[CrossRef\]](#)
27. Torres, R.A.; Nieto, J.I.; Combet, E.; Pétrier, C.; Pulgarin, C. Influence of TiO<sub>2</sub> concentration on the synergistic effect between photocatalysis and high-frequency ultrasound for organic pollutant mineralization in water. *Appl. Catal. B Environ.* **2008**, *80*, 168–175. [\[CrossRef\]](#)
28. Van Doorslaer, X.; Heynderickx, P.M.; Demeestere, K.; Debevere, K.; Van Langenhove, H.; Dewulf, J. Applied Catalysis B: Environmental TiO<sub>2</sub> mediated heterogeneous photocatalytic degradation of moxifloxacin: Operational variables and scavenger study. *Appl. Catal. B Environ.* **2012**, *112*, 150–156. [\[CrossRef\]](#)
29. Sun, H.; He, F.; Choi, W. Production of Reactive Oxygen Species by the Reaction of Periodate and Hydroxylamine for Rapid Removal of Organic Pollutants and Waterborne Bacteria. *Environ. Sci. Technol.* **2020**, *54*, 6427–6437. [\[CrossRef\]](#)
30. Chadi, N.E.; Merouani, S.; Hamdaoui, O.; Bouhelassa, M.; Ashokkumar, M. H<sub>2</sub>O<sub>2</sub>/Periodate (IO<sub>4</sub><sup>−</sup>): A novel advanced oxidation technology for the degradation of refractory organic pollutants. *Water Res. Technol.* **2019**, *5*, 1113–1123. [\[CrossRef\]](#)
31. Hu, Q.; Liu, B.; Zhang, Z.; Song, M.; Zhao, X. Temperature effect on the photocatalytic degradation of methyl orange under UV-vis light irradiation. *J. Wuhan Univ. Technol. Mater. Sci. Ed.* **2010**, *25*, 210–213. [\[CrossRef\]](#)
32. Chatzitakis, A.; Berberidou, C.; Paspaltsis, I.; Kyriakou, G.; Sklaviadis, T.; Poullos, I. Photocatalytic degradation and drug activity reduction of Chloramphenicol. *Water Res.* **2008**, *42*, 386–394. [\[CrossRef\]](#) [\[PubMed\]](#)
33. Yawalkar, A.A.; Bhatkhande, D.S.; Pangarkar, V.G.; Beenackers, A.A.C.M. Solar-assisted photochemical and photocatalytic degradation of phenol. *J. Chem. Technol. Biotechnol.* **2001**, *76*, 363–370. [\[CrossRef\]](#)
34. Bhatkhande, D.S.; Pangarkar, V.G.; Beenackers, A.A.C.M. Photocatalytic degradation for environmental applications—A review. *J. Chem. Technol. Biotechnol.* **2002**, *77*, 102–116. [\[CrossRef\]](#)
35. Fox, M.A.; Dulay, M.T. Heterogeneous Photocatalysis. *Chem. Rev.* **1993**, *93*, 341–357. [\[CrossRef\]](#)
36. Bahnemann, W.; Muneer, M.; Haque, M.M. Titanium dioxide-mediated photocatalysed degradation of few selected organic pollutants in aqueous suspensions. *Catal. Today* **2007**, *124*, 133–148. [\[CrossRef\]](#)
37. Hofstadler, K.; Bauer, R.; Novall, S.; Heisler, G. New Reactor Design for Photocatalytic Wastewater Treatment with TiO<sub>2</sub> Immobilized on Fused-Silica Glass Fibers: Photomineralization of 4-Chlorophenol. *Environ. Sci. Technol.* **1994**, *28*, 670–674. [\[CrossRef\]](#)
38. Andreozzi, R.; Caprio, V.; Insola, A.; Longo, G.; Tufano, V. Photocatalytic oxidation of 4-nitrophenol in aqueous TiO<sub>2</sub> slurries: An experimental validation of literature kinetic models. *J. Chem. Technol. Biotechnol.* **2000**, *75*, 131–136. [\[CrossRef\]](#)
39. Rauf, M.A.; Ashraf, S.S. Fundamental principles and application of heterogeneous photocatalytic degradation of dyes in solution. *Chem. Eng. J.* **2009**, *151*, 10–18. [\[CrossRef\]](#)
40. Moonsiri, M.; Rangsunvigit, P.; Chavadej, S.; Gulari, E. Effects of Pt and Ag on the photocatalytic degradation of 4-chlorophenol and its by-products. *Chem. Eng. J.* **2004**, *97*, 241–248. [\[CrossRef\]](#)
41. Tang, C.; Chen, V. The photocatalytic degradation of reactive black 5 using TiO<sub>2</sub>/UV in an annular photoreactor. *Water Res.* **2004**, *38*, 2775–2781. [\[CrossRef\]](#)
42. Gerischer, H.; Heller, A. The Role of Oxygen in Photooxidation of Organic Molecules on Semiconductor Particles. *J. Phys. Chem.* **1991**, *0*, 5261–5267. [\[CrossRef\]](#)
43. McMurray, T.A.; Dunlop, P.S.M.; Byrne, J.A. The photocatalytic degradation of atrazine on nanoparticulate TiO<sub>2</sub> films. *J. Photochem. Photobiol. A Chem.* **2006**, *182*, 43–51. [\[CrossRef\]](#)
44. Kyoung, N.; Eun, J.; Shim, O.; Lee, H.; Kim, J.; Koun, B. The effect of dissolved oxygen on the 1,4-dioxane degradation with TiO<sub>2</sub> and Au-TiO<sub>2</sub> photocatalysts. *J. Hazard. Mater.* **2010**, *177*, 216–221. [\[CrossRef\]](#)
45. Ohtaki, M.; Sato, H.; Fujii, H.; Eguchi, K. Intramolecularly selective decomposition of surfactant molecules on photocatalytic oxidative degradation over TiO<sub>2</sub> photocatalyst. *J. Mol. Catal. A Chem.* **2000**, *155*, 121–129. [\[CrossRef\]](#)